

On the undulatory behaviour of metallic glass foils: A novel spring-type behaviour

O. Shahin Elzoubi^a, N.T. Panagiotopoulos^b, M. Stiehler^a, K. Salonitis^a,
K. Georgarakis^{a*}

^a School of Aerospace, Transport and Manufacturing, Cranfield University, MK43 0LR, UK

^b Department of Material Science & Metallurgy, University of Cambridge, Cambridge CB3 0FS, UK

* Corresponding author. Tel.: +44 (0) 1234 750111 x5020; E-mail address: k.georgarakis@cranfield.ac.uk

Abstract

The undulatory behaviour is a unique type of mechanical response that was recently observed for metallic glass foils in geometric confinement. It is manifested when normal load is applied on the top of an arc-shaped thin foil of metallic glass; the foil then deforms elastically and its shape changes by progressively increasing the number of formed sinusoidal arcs. This behaviour results from a combination of successive elastic bending and buckling events and can be utilized for developing novel types of non-linear springs. In this work, the undulatory behaviour of a Ni-Fe-Si-B-Mo metallic glass foil has been systematically studied and compared with that of the previously reported Fe-Cr-Si-B foil. The results indicate that the alloy composition and the foil thickness can significantly affect the load required for the formation of the harmonic undulations. The initial geometry of the formed sinusoidal arc including its amplitude and boundary length, can also be used to tune the load and displacement response of the foils. Upon unloading, the foil returns to its initial shape, as long as the loading remains in the elastic deformation range of the metallic glass. The findings suggest that the undulatory behaviour of thin metallic glass foils can be potentially exploited for a wide range of engineering applications including micro-springs, sensors, actuators, and shock absorbers.

Keywords: metallic glass foils; undulatory behaviour; buckling; flat micro-springs

1. Introduction

Metallic glasses are metastable materials with disordered structure and unique properties. They exhibit exceptional mechanical properties, including a high strength higher than 5GPa, good fracture toughness, excellent wear and corrosion resistance and a wide elastic deformation limit of 2% strain [1-5].

Unlike crystalline metals, metallic glasses do not have a periodic lattice with glide planes on which mobile dislocations can cause plastic flow. Due to their exceptional properties, metallic glass thin foils exhibit a unique and reversible sinusoidal mechanical response when load is applied on the top of an elastically shaped arc [6,7], as shown in Fig 1. Consequently, vitrified alloys have been proposed as spring materials with enhanced properties, functioning as flat springs with multiple spring rates [8, 9].

Aljerf et al. [10] found that a metallic glass foil can be formed into complex shapes without embrittlement using thermo-elastic processing (TEP). Under applied load, Fe-based MG foils shaped by TEP revealed a distinctive undulatory behaviour of a fixed number of arcs, which can

support an ultimate load of 270 N in linear spring type of set-ups, while an ultimate load of 450 N in annular spring set-ups [11]. The energy storage capacity of Fe-based MG foils either in linear or annular form is up to 2600 kJ/m³, higher than conventional springs [11].

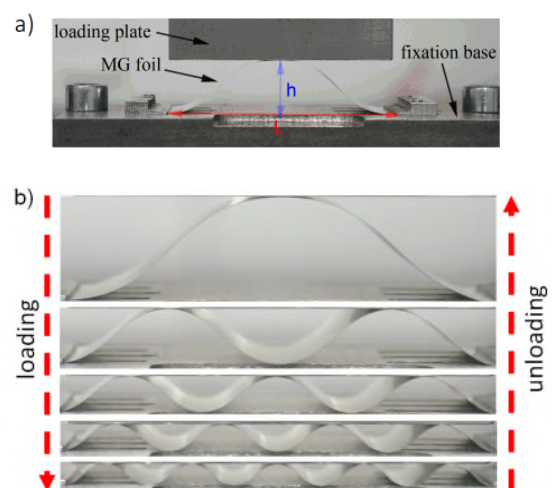


Fig. 1: (a) initial arc-shaped metallic glass foil; (b) harmonic undulatory response of arc-shaped metallic glass foil.

In this communication, we report on the undulatory behaviour of Ni-Fe-Si-B-Mo metallic glass foils for

the first time, and compare with that of the previously reported Fe-Cr-Si-B foil, using a similar methodology as the one proposed in [6]. The undulatory behaviour is affected by factors such as alloy composition (due to difference in elastic/mechanical properties), foil thickness, and initial geometry of the sinusoidal arc including the boundary horizontal length L and arc amplitude.

Nomenclature	
R	radius of arc curvature
W	width of the foils
L	distance between fixation points
h	amplitude
d	thickness of the foil
ε	strain
k	spring rate
MG	metallic glass

2. Experimental details

Two metallic glass alloy foils (commercially available) have been used in this work, namely a) the $\text{Fe}_{76.10}\text{Cr}_{2.48}\text{Si}_{4.51}\text{B}_{16.91}$ (at. %) foil (hereafter referred to as Fe-based) with thickness $d=19\ \mu\text{m}$ and b) $\text{Ni}_{40}\text{Fe}_{40}(\text{SiB})_{19}\text{Mo}_1$ (at. %) (hereafter referred to as NiFe-based alloy) with thickness of $d=25\ \mu\text{m}$. All foils had similar width W of 25 mm.

X-ray diffraction (XRD) was employed to characterize the structure of the foils using a Siemens D5005 with $\text{Cu K}\alpha$ radiation in the 2θ range from 20° to 90° . Differential scanning calorimetry (DSC) using a TA instrument Q200 was employed to investigate the thermal stability of the foils. The measurements were performed in an argon atmosphere using a heating rate of $20^\circ\text{C}/\text{min}$.

An Instron 825 compression machine was employed to apply load on the top of the arc-shaped foils as shown in Fig. 1. A Panasonic DMC-G7 camera was used to film the loading/unloading process and to use these images for analysing local strains on the foils. Load-displacement curves were recorded using initial arc length L values in the range from 20 to 50 mm, initial arc amplitude h in the range from 5 to 12.5 mm and constant ratio of $L/h=4$ as shown in Fig. 1a.

3. Results and discussion

3.1. Structure

Figure 2 show X-ray diffraction patterns taken from the $\text{Fe}_{90.65}\text{Cr}_{2.75}\text{Si}_{2.7}\text{B}_{3.9}$ and $\text{Ni}_{40}\text{Fe}_{40}(\text{SiB})_{19}\text{Mo}_1$ melt spun foils with $19\ \mu\text{m}$ and $25\ \mu\text{m}$ thickness, respectively. Both patterns exhibit only broad-diffuse peaks (around 44° in 2 -theta angle)

indicating their amorphous nature. Fig. 3 presents DSC thermograms of the two amorphous materials studied in this work. For the $\text{Fe}_{90.65}\text{Cr}_{2.75}\text{Si}_{2.7}\text{B}_{3.9}$ foil, an exothermic peak with onset at $T_x = 520^\circ\text{C}$ is observed, corresponding to the crystallization of the amorphous phase. For the $\text{Ni}_{40}\text{Fe}_{40}(\text{SiB})_{19}\text{Mo}_1$ alloy, crystallization occurs around 455°C , whereas a second crystallization reaction occurs around 525°C .

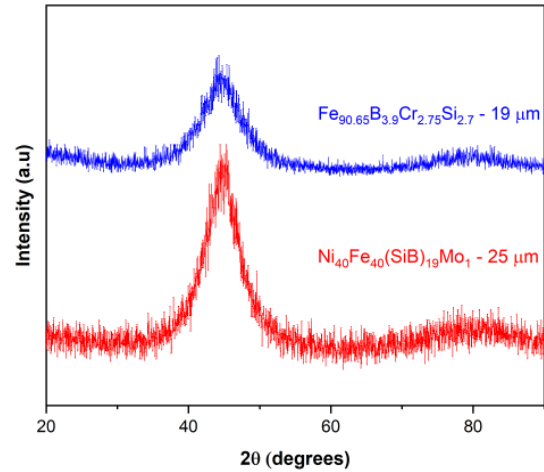


Fig. 2. X-ray diffraction patterns of the metallic glass foils.

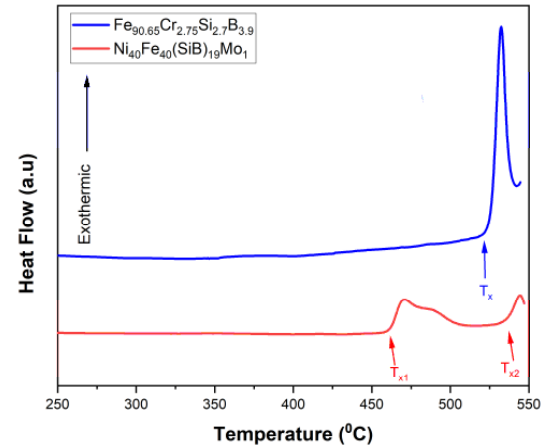


Fig. 3. DSC thermograms of the metallic glass foils

3.2. Undulatory behaviour

Mechanical loading was applied on the top of arc-shaped Fe-based and NiFe-based foils as shown in Fig. 1. Upon loading, the foils deform elastically up to a specific value of load or displacement, followed by a change in their shape leading to a successive increase of the number of sinusoidal arcs, Fig. 1b. Fig. 4a presents the load versus displacement for the Fe-based MG foil with boundary distance $L=20\ \text{mm}$, amplitude of the initial arc $h_1=5\ \text{mm}$ (aspect ratio) $h_1=L/4$, Fig. 1a. As expected, the results in Fig. 4a indicate similar undulatory behaviour with that shown by Panagiotopoulos et al [6]. During loading,

the load-displacement curves can be overall described by exponential relations of the type $F = \alpha \cdot \exp(\beta x)$ but with discrete discontinuities at specific values of displacement. Where α and β are constants (depended on the initial arc geometry and materials) and x is the displacement, The discontinuities, represented by small but sharp load decrease, occur at the time of the formation of additional arcs. In between these abrupt drops in load, one could approach the segments of the curve as quasi-linear, with the slopes considered equivalent to the spring rate k according to Hooke's law. Overall, due to the undulatory behaviour, arc-shaped metallic glass foils subjected to loading conditions (Fig. 1), operate as non-linear flat springs with variable spring's rates [6, 7].

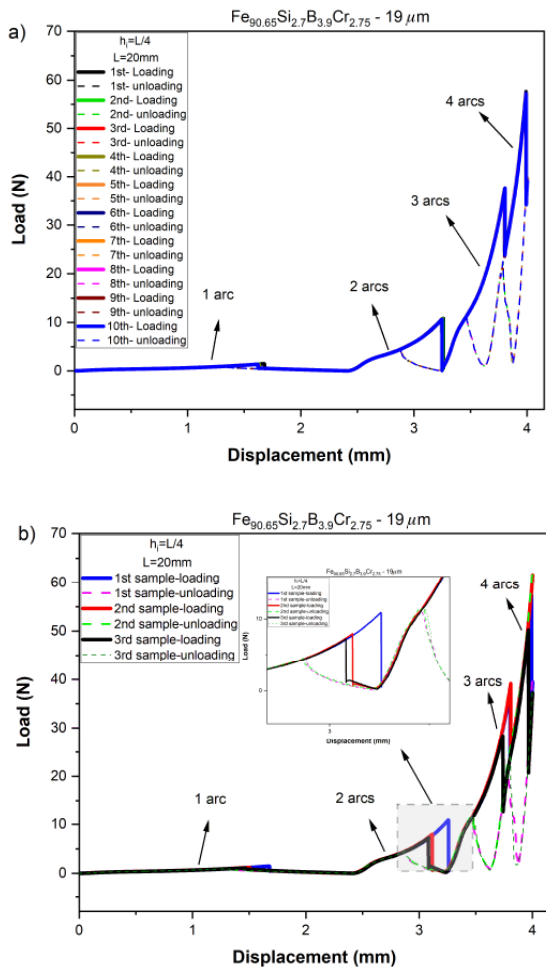


Fig. 4: (a) Load-displacement curves for ten cycles loading/unloading of a foil; (b) load-displacement curves on three samples of Fe-based metallic glass foils

Figure 4a shows ten (10) successive loading cycles for the same foil to follow the exact same path, highlighting the repeatability of the undulatory behaviour. During unloading, the load-displacement path shows a hysteresis compared to the loading

path, but yet identical for all unloading cycles; returning however to the exact initial shape and position as the initial sinusoidal arc.

Figure 4b shows the load displacement response of three samples of the same material (Fe-based foil) and same initial arc geometry. The three samples follow essentially the same path showing the same behaviour as expected, confirming the repeatability of the process. Some minor variations at the position of the sharp load drop can be observed, whereas the paths exactly coincide again when loading resumes, as shown in the insert of Fig. 4b.

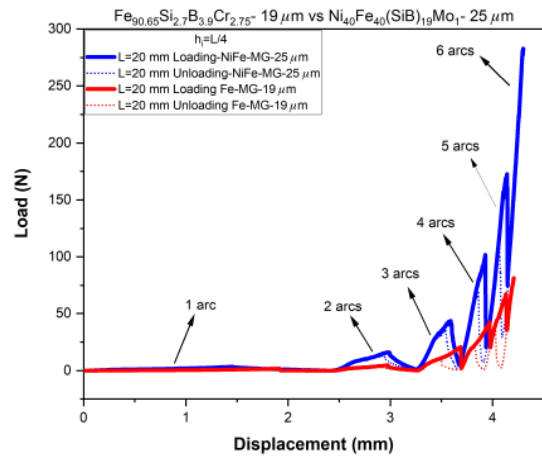


Fig. 5. Load-displacement curves upon loading for the NiFe-based (25 μm thick, blue) metallic glass foil compared to the Fe-based one (19 μm thick, red) for $L=20$ mm and $h_l=5$ mm.

Figure 5 presents the load-displacement curve upon loading and unloading for an arc-shaped NiFe-based (25 μm thick) metallic glass foil -for the first time- in comparison with the Fe-based one (19 μm thick) for $L=20$ mm and $h_l=5$ mm. A similar behaviour can be observed for the two amorphous foils, as expected, where the load increases quasi-exponentially with increasing distance. The arc multiplication occurs at about the same displacement values for both foils, but clearly, the NiFe-based foil exhibits higher load values compared to the Fe-based one. For example, the transition from 2 to 3 arcs the NiFe-based foil requires around 16 N whereas for the thinner Fe-foil only 5 N while the transition from 4 to 5 arcs requires 100 N compared with Fe-based MG foil that requires 42 N. For higher order transitions the load differences are even higher. This indicates that with the appropriate choice of the thickness of the foils as well as the metallic glass alloy –in terms of Young's modulus – one can effectively design non-linear flat spring type devices with desirable mechanical response. Further work is currently underway to model the effect of foil thickness on the mechanical

undulatory response of the metallic glass foils. Focusing on the unloading cycle, again, a “hysteresis” is observed in the unloading cycle, in both cases, while the foil returns to the initial position and resuming the initial sinusoidal arc shape.

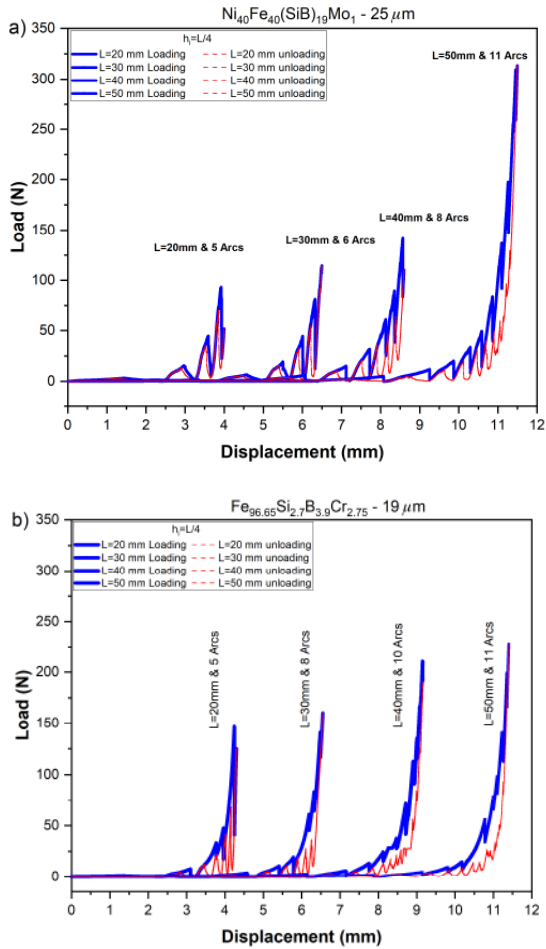


Fig. 6: (a) Load-displacement curves for the NiFe-based (25 μm thick) metallic glass foil for boundary distance L values in the range of 20–50 mm and h_1 to L ratio $h_1/L=0.25$; (b) Load-displacement curves for the Fe-based (19 μm thick) metallic glass foil.

Figures 6a and 6b depict the load-displacement curves for boundary distance L values in the range of 20–50 mm and h_1 to L ratio $h_1/L=0.25$ for NiFe-based (25 μm thick) and the Fe-based glassy foils respectively. Spring type set-ups with higher L values can reach higher number of arcs (while still within the elastic deformation limit of 2% for the metallic glass foils) as well as higher load and displacement values. Thus, the geometry and size of the initial sinusoidal arc gives another design tool to tune the range of the mechanical responses of these types of spring-type set-ups or devices.

Figure 7a shows the load required to induce the transition from n_i sinusoidal arcs to the $n_i + 1$ arc

versus the number of arcs for the Fe-based and NiFe-based metallic glass foils with initial arc geometry defined by L values in the range of 20–50 mm and initial amplitude h_1 to L ratio $h_1/L=0.25$. Comparing the two foils, the load for the NiFe-based foils is higher than that for the thinner Fe-foils as inferred from Fig. 6a and 6b. Comparing the initial boundary length L , higher L values lead to lower load for the same number of arcs. However, the glassy foil set-ups with higher L values can allow the formation of higher number of arcs while remaining in the region of elastic deformation of the metallic glass foils and thus able to reach considerably higher load values.

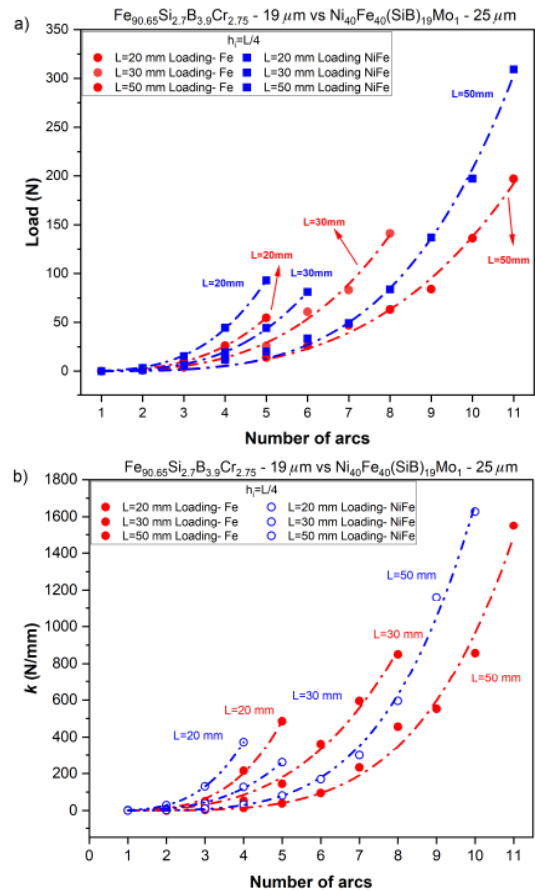


Fig. 7: (a) Maximum applied normal load on the foils with n_i sinusoidal arcs just before the formation of the $n_i + 1$ arc versus the number of arcs for the Fe-based and NiFe-based metallic glass foils for set-ups with boundary distance L values in the range of 20–50 mm and h_1 to L ratio $h_1/L=0.25$; (b) the spring rates (k) as calculated in the quasi-linear segments of the load-displacement curves. Values for $L=40$ mm were omitted for the clarity of the graphs.

Figure 7b shows the calculated spring rate versus the number of arcs for different boundary lengths (L) for both type of glassy foils. Similarly, the spring rate k values show exponential increase with the increase of the number of arcs. For initial foil set-up with

higher L values this increase of is more gradual in the beginning but can reach higher number arcs and higher k values. Furthermore, the Ni-Fe foils exhibit higher k values compared to the thinner Fe based alloy. Characteristically, for the Ni-Fe based foil at $L=50$ mm, the estimated spring rate range from about 1 to 1600 N/mm depending on the number of the formed arcs, and the horizontal boundary conditions L . Thus, the NiFe-based MG foil is shown higher load values and spring rate values mainly due to its higher thickness compared to Fe-based MG foil.

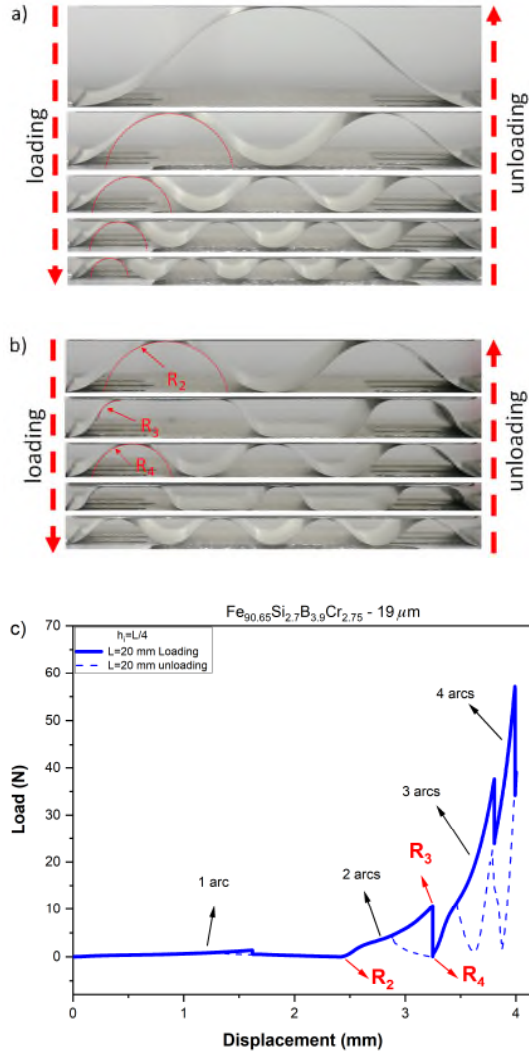


Fig. 8: (a) Assembly of snapshots from the undulatory response of a metallic glass foil with images of waveforms with perfect sinusoidal shaped arcs; (b) assembly of snapshots from the undulatory response with images of waveforms with perfect sinusoidal shaped arcs (R_2 and R_4) and distorted arcs (R_3), and; (c) load-displacement curve of the undulatory response for the Fe-based foil.

3.3 Estimation of local strain

For the undulatory behaviour to remain reversible and repeatable, plastic deformation must be avoided.

Thus, the strain must always remain below 2% which is the limit of elastic deformation in metallic glasses. As the foil undergoes deformation and bending phenomena, the strain is not homogeneously distributed in the foil; it rather becomes maximum locally at positions that exhibit “highest bending” or the smallest radius of curvature. We have previously considered [6] the local strains at the waveforms with perfectly shaped sinusoidal arcs, as shown in Fig. 8a. However, a close observation of the evolution of the foil’s geometry Fig. 8b, reveals that the radius of curvature is smallest just before the formation of a new (n_i+1) arc (R_3 in Fig. 8b) rather than when an additional arc is formed see R_2 and R_4 in Fig. 8b and thus the strain needs to be primarily considered at this step of the shape evolution of the foil. These states of the foil’s shape evolution are indicated in the load displacement curve of Fig. 8c. Thus, between R_3 and R_4 the transition from two to three arcs occurs accompanied by a drop in load.

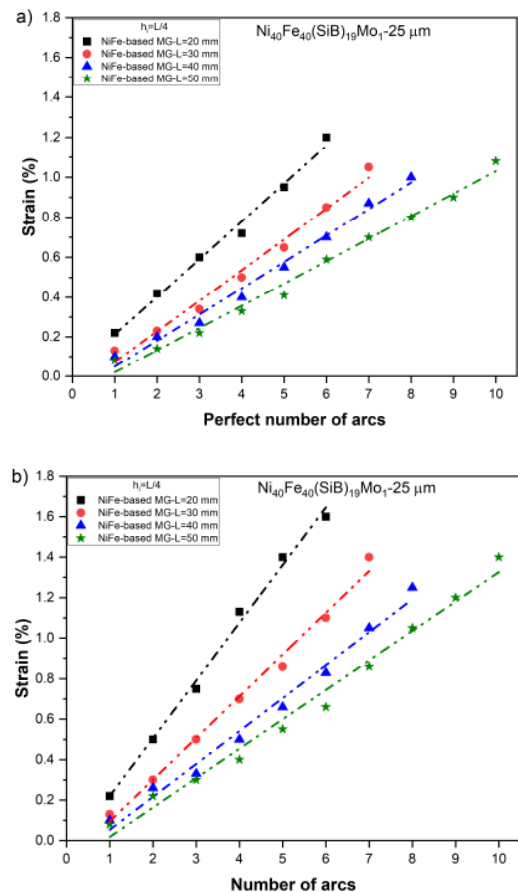


Fig. 9: Maximum local strain on the foils (a) at waveforms with perfectly shaped sinusoidal arcs (equivalent to R_2 and R_4 in the example of Fig. 8b); (b) at waveform with distorted arcs, just before the formation of a new (n_i+1) arc (equivalent to R_3 in the example of Fig. 8b).

Figure 9a presents the local strain on the foils at the steps where perfect sinusoidal arcs are formed, equivalent to R_2 and R_4 in Fig. 8b for the Ni-Fe metallic glass foil with a variety of initial boundary lengths between $L=20$ mm and $L=50$ mm. Fig. 9b presents the estimated local strains foils at the steps of maximum distortion, equivalent to R_3 in Fig. 8b for similar conditions as in Fig. 9a. In both cases and all represented measurements, the local strain remains below the 2% limit of elastic deformation.

To sum up, the work studied the undulatory behaviour of a metallic glass system that was not previously investigated. The results confirm previous observations on a different alloy system on one hand and on the other hand, uncover the remarkable repeatability of the undulations under cycling conditions. The findings clearly evidence the potential of this extraordinary behaviour to be exploited in spring-type applications. The choice of the glassy alloy and the thickness of the foil is shown to enable the tuning of the mechanical response of the foil under loading and thus enriching the capabilities for designing spring-type devices with desirable characteristics that can efficiently operate in different load ranges. Overall, the work significantly contributes to the understanding of the recently discovered undulatory mechanical response and clarifies the operational limitations imposed by local deformation.

4. Conclusions

The undulatory behaviour of metallic glass foils was investigated for Ni-Fe-based and Fe based alloy foils of different thicknesses. For both alloys, the initially arc shaped foils deform elastically creating harmonic wavy patterns, in a reversible and repeatable manner, similar to a non-linear spring-type behaviour. The results indicate that the thickness of the foils as well as the choice of the glassy alloy affect the load required for the transition from a lower order (n_i arcs) to higher order (n_i+1 arcs) waveform.

The initial geometry of the formed sinusoidal arc, like the boundary length L and initial amplitude h also influence the load and displacement response of the foils and thus can be used for tuning the spring-type behaviour of the set-up. The thicker Ni-Fe-based foils showed higher load for the same distance (or number of arcs formed) as well as higher springs' rate values compared to the thinner Fe based foils. Under the conditions examined in this study, the foils always remain in the elastic deformation region. Remaining always below this elastic limit (2% strain for metallic glasses) is critical for the reversibility of this behaviour.

Acknowledgement

OSE acknowledges support from Libyan Ministry of Higher Education & Scientific Research via Libyan Academic Attaché - London. Support from EPSRC-DTP project on "Bulk Metallic Glasses" (ref. 2043971) is gratefully acknowledged.

References

- [1] Inoue, A. (2000) 'Stabilization of metallic supercooled liquid and bulk amorphous alloys', *Acta Materialia*, 48(1), pp. 279–306. doi: 10.1016/S1359-6454(99)00300-6.
- [2] Ashby, M. F. and Greer, A. L. (2006) 'Metallic glasses as structural materials', *Scripta Materialia*, 54(3), pp. 321–326. doi: 10.1016/j.scriptamat.2005.09.051.
- [3] Yavari, A. R. (2006) 'A new order for metallic glasses', *Nature*, 439, pp. 405–406.
- [4] Pang, S. J., Zhang, T., Asami, K. and Inoue, A. (2002) 'Synthesis of Fe-Cr-Mo-C-B-P bulk metallic glasses with high corrosion resistance', *Acta Materialia*, 50(3), pp. 489–497. doi: 10.1016/S1359-6454(01)00366-4.
- [5] Georganakakis, K., Aljerf, M., Li, Y., Lemoulec, A., Charlot, F., Yavari, A. R., Chornokhvostenko, K., Tabachnikova, E., Evangelakis, G. A., Miracle, D. B., Greer, A. L. and Zhang, T. (2008) 'Shear band melting and serrated flow in metallic glasses', *Applied Physics Letters*, 93(3), pp. 2–5. doi: 10.1063/1.2956666.
- [6] Panagiotopoulos, N. T., Yousfi, M. A., Georganakakis, K. and Yavari, A. R. (2016) 'Mechanically induced waves in metallic glass foils', *Materials and Design*, 90, pp. 1110–1114. doi: 10.1016/j.matdes.2015.10.149.
- [7] Yousfi, M. A., Panagiotopoulos, N. T., Jorge Junior, A. M., Georganakakis, K. and Yavari, A. R. (2017) 'Novel micro-flat springs using the superior elastic properties of metallic glass foils', *Scripta Materialia*, 131, pp. 84–88. doi: 10.1016/j.scriptamat.2017.01.012.
- [8] Son, K., Soejima, H., Nishiyama, N., Wang, X. M. and Inoue, A. (2007) 'Process development of metallic glass wires by a groove quenching technique for production of coil springs', *Materials Science and Engineering A*, 448–451, pp. 248–252. doi: 10.1016/j.msea.2006.02.309.
- [9] Chan, K. C. and Sort, J. (2015) 'Metallic glasses', *Metals*, 5(4), pp. 2397–2400. doi: 10.3390/met5042397.
- [10] Aljerf, M., Georganakakis, K. and Yavari, A. R. (2011) 'Shaping of metallic glasses by stress-annealing without thermal embrittlement', *Acta Materialia*. Acta Materialia Inc., 59(10), pp. 3817–3824. doi: 10.1016/j.actamat.2011.02.039.
- [11] Panagiotopoulos, N. T., Georganakakis, K., Jorge, A. M., Aljerf, M., Botta, W. J., Greer, A. L. and Yavari, A. R. (2020) 'Advanced ultra-light multifunctional metallic-glass wave springs', *Materials and Design*. Elsevier Ltd, 192, p. 108770. doi: 10.1016/j.matdes.2020.108770.